Journal of Organometallic Chemistry, 389 (1990) 361–374
Elsevier Sequoia S.A., Lausanne – Printed in The Netherlands
JOM 20808

Linkage of two trimetallic clusters through the bridging ligands C_3HO_2 and C_3O_2. Crystal structures of three clusters containing the components $Os_3CHCCO_2Os_3$, $Ru_3CHCCO_2Os_3$, and $Os_3CCCO_2Os_3$

Kenneth I. Hardcastle *, Tim McPhillips,

Department of Chemistry, California State University Northridge, 18111 Nordhoff Street, Northridge, California 91330 (U.S.A.)

Alejandro J. Arce *, Ysaura De Sanctis,

Instituto Venezolano de Investigaciones Cientificas, Chemistry Center, Apartado 21827, Caracas 1020-A (Venezuela)

Antony J. Deeming * and Nicholas I. Powell

Department of Chemistry, University College London, 20 Gordon Street, London WC1H OAJ (U.K.)

(Received December 7th, 1989)

Abstract

Reaction of propynoic acid ($CH{\equiv}CCO_2H$) with $[Os_3(CO)_{10}(MeCN)_2]$ gives the species $[Os_3H(CH{\equiv}CCO_2)(CO)_{10}]$ containing a μ-carboxylato ligand and a non-coordinated acetylenic function which may be coordinated further. Reaction of this compound with $[M_3(CO)_{10}(MeCN)_2]$ (M = Os or Ru) gives the linked cluster compounds $[Os_3(CO)_{10}(CH{\equiv}CCO_2)Os_3H(CO)_{10}]$ (**1**) and $[Ru_3(CO)_{10}(CH{\equiv}CCO_2)Os_3H(CO)_{10}]$ (**2**), the crystal structures of which are reported. A comparison of the geometries of the compounds $[M_3(CO)_{10}(alkyne)]$ (M = Os or Ru) is possible for the first time; each contains a μ-CO ligand, which is more symmetrical for M = Ru than for M = Os. The coordination geometries of the μ_3-alkyne and the overall conformations of the linked clusters are very similar. Decarbonylation of **1** and **2** leads to $[Os_3H(CO)_9(C_3O_2)Os_3H(CO)_{10}]$ (**3**) (crystal structure reported) and $[Ru_3H(CO)_9(C_3O_2)Os_3H(CO)_{10}]$ (**4**) respectively.

Introduction

In an earlier paper on the chemistry of alkynes with oxyfunctions such as CHO or CO_2H we described the linkage of two trinuclear clusters through the ligand

0022-328X/90/$03.50 © 1990 – Elsevier Sequoia S.A.

μ_5-CH≡CCO$_2$ starting from propynoic acid and [M$_3$(CO)$_{10}$(MeCN)$_2$] (M = Os or Ru) [1]. In this paper we describe the crystal structures of three linked clusters and, in particular, compare the coordination geometries of the alkyne function in its attachment to the metal carbonyl units Os$_3$(CO)$_{10}$ and Ru$_3$(CO)$_{10}$. The crystal structures of [Os$_3$(CO)$_{10}$(alkyne)] have been reported elsewhere where alkyne = PhC$_2$Ph [2], HC$_2$Fc (Fc = ferrocenyl) [3], and EtC$_2$Et [4] and the structure of [Os$_3$(EtC$_2$Et)(CO)$_9$(PPh$_3$)] [4] is also known: however no triruthenium cluster of this class has been structurally characterised previously. Indeed it was not until [Ru$_3$(CO)$_{10}$(MeCN)$_2$] had been synthesised [5] that the triruthenium alkynes were available since the direct reactions of [Ru$_3$(CO)$_{12}$] with alkynes do not yield [Ru$_3$(CO)$_{10}$(alkyne)]. It was reported that the reaction of [Ru$_3$(CO)$_{10}$(MeCN)$_2$] with the terminal alkyne PhC$_2$H gives the decarbonylation product [Ru$_3$H(C$_2$Ph)(CO)$_9$] [5]. Simple decacarbonyl species of the kind [Ru$_3$(CO)$_{10}$(alkyne)] do not seem to have been synthesised previously by this route. We have found that the bis-acetontitrile-triruthenium compound is very unstable in solution and successful reactions seems to require addition of the solid cluster to a solution containing the other reagent, so that reaction occurs instantly on dissolution, rather than addition of the reagent to a prepared solution of [Ru$_3$(CO)$_{10}$(MeCN)$_2$]. Very recently the clusters [Ru$_3$(CO)$_{10}$(alkyne)] have been synthesised from [PPN][Ru$_3$Cl(CO)$_{10}$] via the alkyne cluster [PPN][Ru$_3$Cl(alkyne)(CO)$_9$], the chloride ion being displaced by CO in the presence of protic solvents [6].

Results and discussion

Syntheses. The bis-acetonitrile compound [Os$_3$(CO)$_{10}$(MeCN)$_2$] reacts with alkynes (RC$_2$H) to give the alkyne clusters [Os$_3$(CO)$_{10}$(RC$_2$H)] and with carboxylic acids (RCO$_2$H) to give the carboxylato complexes [Os$_3$H(RCO$_2$)(CO)$_{10}$] so that in principle propynoic acid (CH≡CCO$_2$H) could react in either way. However, the product is clearly identified spectroscopically as the oxidative addition compound [Os$_3$H(CH≡CCO$_2$)(CO)$_{10}$] with the ligand coordinated through the carboxylate group [1]. The IR spectrum is very similar to those of related carboxylato compounds such as [Os$_3$H(HCO$_2$)(CO)$_{10}$] [7]. The ^{1}H NMR spectrum shows a hydride signal and the acetylenic hydrogen chemical shift is very little different from that of the free ligand. Curiously propynoic acid reacts with [Ru$_3$(CO)$_{10}$(MeCN)$_2$] to give [Ru$_3$(CO)$_{10}$(μ_3-CH≡CCO$_2$H)] [8]. It could be that the osmium analogue of this cluster is formed first and that isomerisation involving oxidative addition occurs subsequently. However, we do not think that this is the case because ruthenium compounds are generally more reactive than their osmium counterparts and there is no reason why the alkyne-Ru$_3$ cluster would not isomerise to [Ru$_3$H(CH≡CCO$_2$)(CO)$_{10}$] if this were the case. It seems more likely that the triruthenium species is intrinsicially more reactive than the triosmium species towards alkynes than towards carboxylic acids.

The compound [Os$_3$H(CH≡CCO$_2$)(CO)$_{10}$] reacts readily with [Os$_3$(CO)$_{10}$(MeCN)$_2$] within 1 min in dichloromethane at room temperature to give [Os$_3$(CO)$_{10}$(CH≡CCO$_2$)Os$_3$H(CO)$_{10}$] (**1**) and with [Ru$_3$(CO)$_{10}$(MeCN)$_2$] also in dichloromethane but at −20 °C to give [Ru$_3$(CO)$_{10}$(CH≡CCO$_2$)Os$_3$H(CO)$_{10}$] (**2**) (see Scheme 1). As indicated in the Introduction best yields of **2** were obtained by the addition of solid bis-acetonitrile triruthenium compound to a solution of

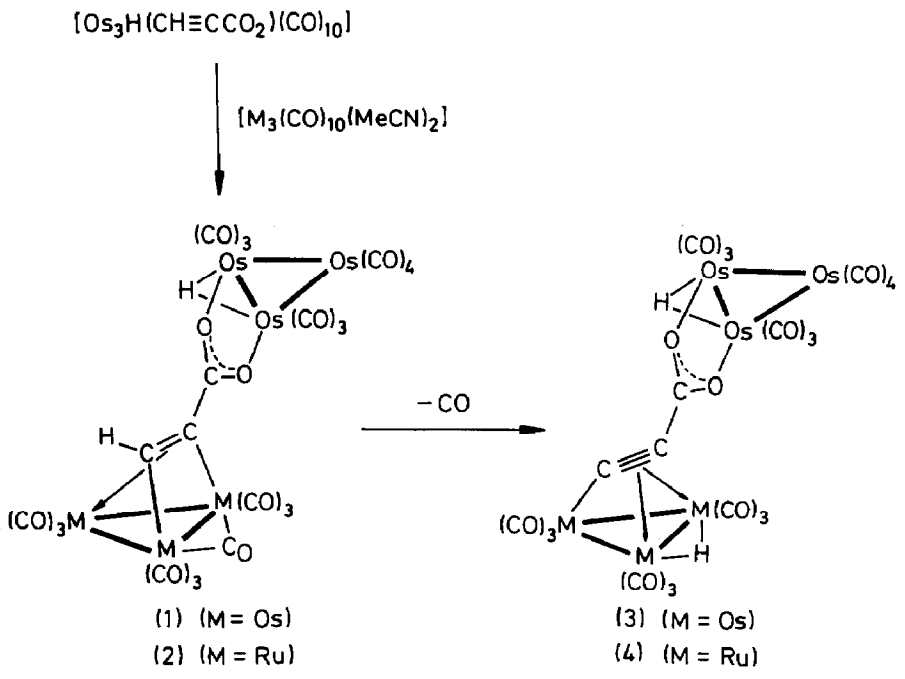

Scheme 1

$[Os_3H(CH{\equiv}CCO_2)(CO)_{10}]$ in dichloromethane. Compounds **1** and **2** can be easily isolated as red and orange crystals, respectively. The IR and NMR spectra appear to be a combination of those of the individual cluster components. Compound **1** gives two ^1H NMR singlets at δ 10.1 and -10.5 for the organic and hydridic hydrogen atoms, respectively. The acetylenic proton signal has shifted from δ 2.8 in the parent cluster to the much lower field characteristic of a μ_3-alkyne whereas the metal hydride shift is unchanged on formation of **1** as expected. The corresponding shifts for **2** are δ 9.0 and -10.6.

Thermal treatments of compounds **1** and **2** in refluxing octane or cyclohexane respectively give the like compounds **3** and **4** containing bridging μ_5-C_3O_2 ligands. The ^1H NMR spectrum of each product contains two hydride signals at δ -10.4 for the $Os_3H(RCO_2)(CO)_{10}$ components and at δ -23.2 and -21.15 which are characteristic of the μ_3-alkynyl components $Os_3H(RC_2)(CO)_9$ and $Ru_3H(RC_2)(CO)_9$, respectively. No other products could be detected and the yields of **3** and **4** seem to be essentially quantitative although, since the reactions were carried out on a small scale, this was not established very carefully. There seems to be no doubt about the nature of the linked clusters **1** to **4** but we have determined the single-crystal X-ray structures of **1** to **3** to compare the geometries of $[M_3(CO)_{10}$(alkyne)] clusters since ruthenium compounds of this kind had not been structurally characterised previously. Also in general terms we wanted to see if the close approach of two ligand-linked clusters would lead to any interesting geometric effects. We wanted to know, for example, if the CO ligands of adjacent clusters were close enough to intermesh and whether this might have an effect on the favoured conformation about the central $C{-}CO_2$ bond, perhaps leading to restricted rotation.

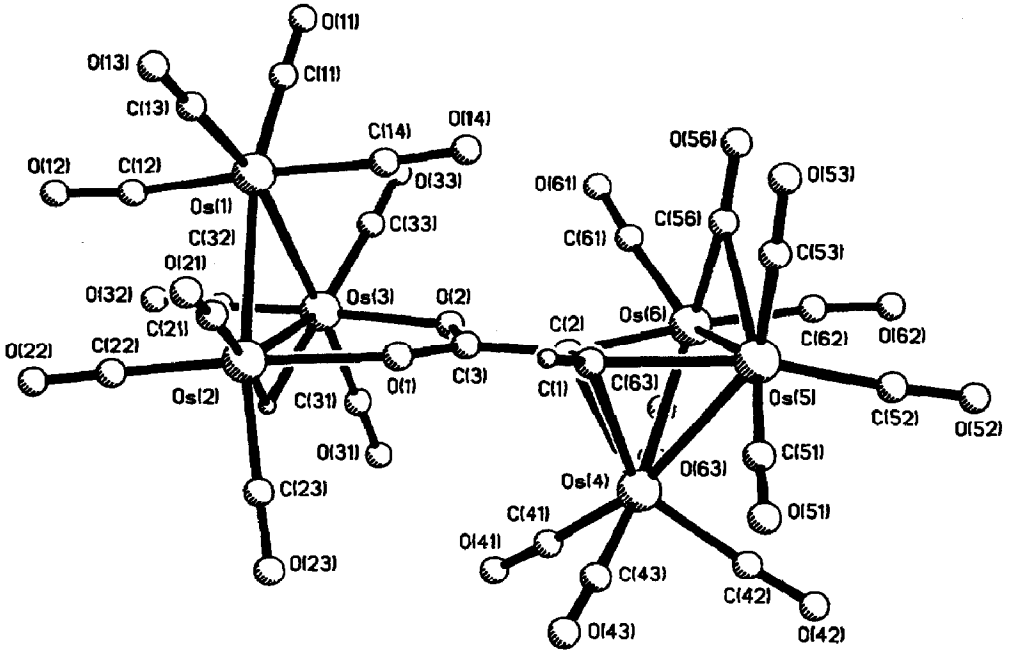

Fig. 1. Molecular structure of $[Os_3(CO)_{10}(C_3HO_2)Os_3H(CO)_{10}]$ (**1**).

Crystal structures. The molecular structures of compounds **1** to **3** found in their crystals are shown in Fig. 1 to 3 and selected bond lengths and angles are in Tables 1 to 3. Compounds **1** and **2** are structurally very similar. The geometries of the $Os_3H(RCO_2)(CO)_{10}$ units in each are essentially indistinguishable and very much like the geometry of $[Os_3H(HCO_2)(CO)_{10}]$ [6]. The $CHCCO_2$ ligands in **1** and **2** are

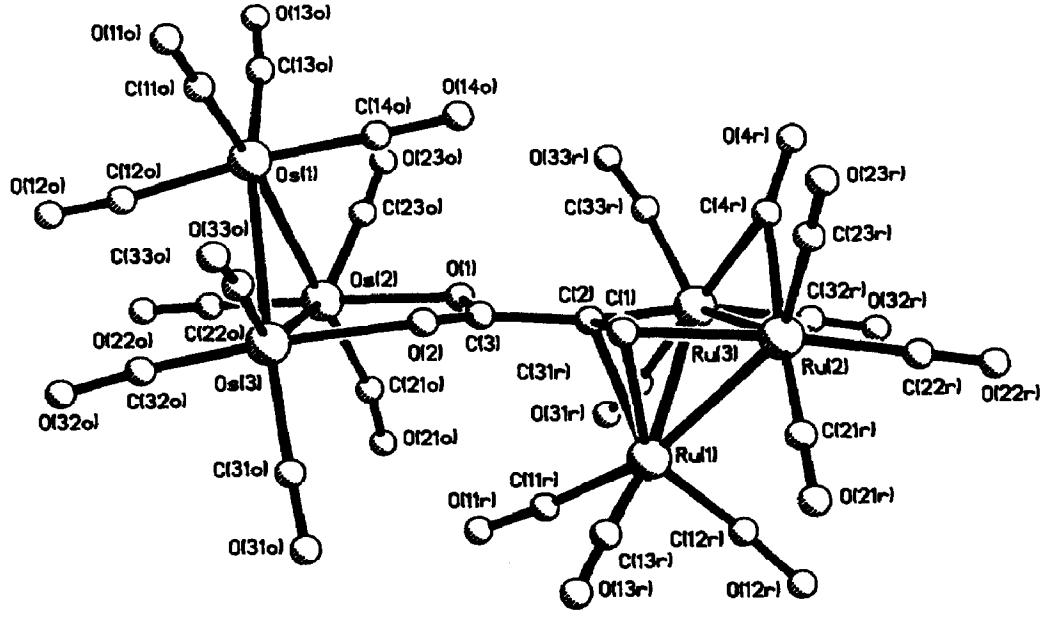

Fig. 2. Molecular structure of $[Ru_3(CO)_{10}(C_3HO_2)Os_3H(CO)_{10}]$ (**2**).

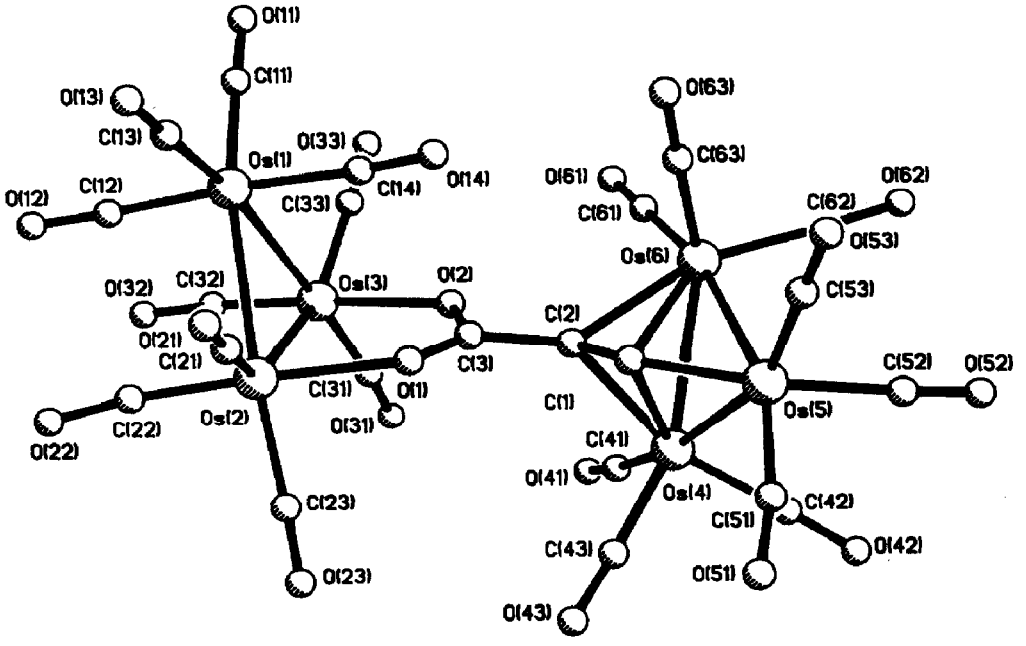

Fig. 3. Molecular structure of $[Os_3H(CO)_9(C_3O_2)Os_3H(CO)_{10}]$ (3).

close to planar which would allow effective p_π–p_π bonding between C(2) and C(3). The CO ligands of the adjacent trinuclear clusters are in fact far enough apart to have no effect on the conformations about the C(2)–C(3) bonds. The most interesting features of the two structures relate to the geometries of the $M_3(CO)_{10}$(alkyne) groups. Although the alkyne adopts the expected parallel arrangement in each, there

Table 1

Selected bond lengths (Å) and angles (°) for $[Os_3(CO)_{10}(C_3HO_2)Os_3H(CO)_{10}]$ (1)

Os(1)–Os(2)	2.851(1)	Os(4)–Os(5)	2.752(1)
Os(2)–Os(3)	2.910(1)	Os(5)–Os(6)	2.862(1)
Os(1)–Os(3)	2.860(1)	Os(4)–Os(6)	2.789(1)
Os(2)–O(1)	2.12(2)	Os(5)–C(1)	2.13(2)
Os(3)–O(2)	2.14(2)	Os(6)–C(2)	2.11(2)
C(3)–O(1)	1.27(2)	Os(4)–C(1)	2.27(2)
C(3)–O(2)	1.28(2)	Os(4)–C(2)	2.17(2)
C(2)–C(3)	1.46(3)	Os(5)–C(56)	2.46(2)
C(1)–C(2)	1.40(2)	Os(6)–C(56)	1.98(2)
Os(1)–Os(2)–O(1)	89.7(4)	C(1)–C(2)–Os(6)	112(2)
Os(1)–Os(3)–O(2)	92.1(3)	C(2)–C(1)–Os(5)	108(1)
Os(2)–Os(3)–O(2)	80.9(2)	Os(6)–Os(5)–C(1)	70.1(4)
Os(3)–Os(2)–O(1)	80.7(3)	Os(5)–Os(6)–C(2)	69.4(5)
Os(3)–O(2)–C(3)	127(1)	Os(4)–C(1)–Os(5)	77.4(8)
Os(2)–O(1)–C(3)	128(1)	Os(4)–C(2)–Os(6)	81.4(8)
O(1)–C(3)–O(2)	123(1)	C(1)–Os(5)–Os(4)	53.6(5)
O(2)–C(3)–C(2)	118(2)	C(2)–Os(6)–Os(4)	50.2(5)
O(1)–C(3)–C(2)	119(2)	Os(5)–C(56)–Os(6)	79.5(8)
C(1)–C(2)–C(3)	118(2)	Os(6)–C(56)–O(56)	156(2)
C(3)–C(2)–Os(6)	129(1)	Os(5)–C(56)–O(56)	125(1)

Table 2

Selected bond lengths (Å) and angles (°) for $[Ru_3(CO)_{10}(C_3HO_2)Os_3H(CO)_{10}]$ (2)

Os(1)–Os(2)	2.870(1)	Ru(1)–Ru(2)	2.738(3)
Os(2)–Os(3)	2.902(1)	Ru(2)–Ru(3)	2.828(4)
Os(1)–Os(3)	2.864(1)	Ru(1)–Ru(3)	2.747(3)
Os(2)–O(1)	2.15(2)	Ru(2)–C(1)	2.11(2)
Os(3)–O(2)	2.12(2)	Ru(3)–C(2)	2.08(3)
C(3)–O(1)	1.30(2)	Ru(1)–C(1)	2.25(3)
C(3)–O(2)	1.24(2)	Ru(1)–C(2)	2.17(3)
C(2)–C(3)	1.55(3)	Ru(2)–C(4r)	2.26(3)
C(1)–C(2)	1.38(2)	Ru(3)–C(4r)	2.04(3)
Os(1)–Os(2)–O(1)	93.9(4)	C(1)–C(2)–Ru(3)	114(2)
Os(1)–Os(3)–O(2)	90.4(6)	C(2)–C(1)–Ru(2)	107(1)
Os(2)–Os(3)–O(2)	80.9(6)	Ru(3)–Ru(2)–C(1)	70.9(8)
Os(3)–Os(2)–O(1)	82.5(5)	Ru(2)–Ru(3)–C(2)	68.5(8)
Os(3)–O(2)–C(3)	125(2)	Ru(1)–C(1)–Ru(2)	77.7(9)
Os(2)–O(1)–C(3)	121(2)	Ru(1)–C(2)–Ru(3)	80.5(9)
O(1)–C(3)–O(2)	129(2)	C(1)–Ru(2)–Ru(3)	70.9(8)
O(2)–C(3)–C(2)	117(2)	C(2)–Ru(3)–Ru(2)	68.5(8)
O(1)–C(3)–C(2)	113(2)	Ru(2)–C(4r)–Ru(3)	82(1)
C(1)–C(2)–C(3)	117(3)	Ru(3)–C(4r)–O(4r)	143(3)
C(3)–C(2)–Ru(3)	129(2)	Ru(2)–C(4r)–O(4r)	134(3)

is some distortion from the symmetrical geometry. Thus in the η^2-coordination Os(4)–C(1) is longer than Os(4)–C(2) and likewise Ru(1)–C(1) is longer than Ru(1)–C(2). These differences are not strongly significant when judged in terms of the e.s.d's but are found in all the structures of this type so far determined, that is in

Table 3

Selected bond lengths (Å) and angles (°) for $[Os_3H(CO)_9(C_3O_2)Os_3H(CO)_{10}]$ (3)

Os(1)–Os(2)	2.8585(7)	Os(4)–Os(5)	2.8598(5)
Os(2)–Os(3)	2.9044(7)	Os(5)–Os(6)	2.8544(8)
Os(1)–Os(3)	2.8708(7)	Os(4)–Os(6)	2.8258(7)
Os(2)–O(1)	2.129(9)	Os(4)–C(1)	2.24(1)
Os(3)–O(2)	2.154(9)	Os(4)–C(2)	2.21(1)
C(3)–O(1)	1.26(1)	Os(6)–C(1)	2.24(1)
C(3)–O(2)	1.23(2)	Os(6)–C(2)	2.18(1)
C(2)–C(3)	1.46(2)	Os(5)–C(1)	1.93(1)
C(1)–C(2)	1.32(2)		
Os(1)–Os(2)–O(1)	92.5(2)	C(3)–C(2)–Os(4)	128.1(9)
Os(1)–Os(3)–O(2)	93.7(2)	C(2)–C(1)–Os(5)	150.2(9)
Os(2)–Os(3)–O(2)	80.9(2)	C(2)–C(1)–Os(4)	71.9(7)
Os(3)–Os(2)–O(1)	80.7(2)	C(2)–C(1)–Os(6)	70.1(7)
Os(3)–O(2)–C(3)	125.5(8)	C(1)–Os(5)–Os(4)	51.3(3)
Os(2)–O(1)–C(3)	125.9(9)	C(1)–Os(5)–Os(6)	51.5(3)
O(1)–C(3)–O(2)	126(1)	C(2)–Os(6)–Os(4)	50.5(3)
O(2)–C(3)–C(2)	118(1)	C(2)–Os(4)–Os(6)	49.4(3)
O(1)–C(3)–C(2)	116(1)	C(1)–Os(4)–C(2)	34.5(5)
C(1)–C(2)–C(3)	139(1)	C(1)–Os(6)–C(2)	34.8(5)
C(3)–C(2)–Os(6)	135.9(8)		

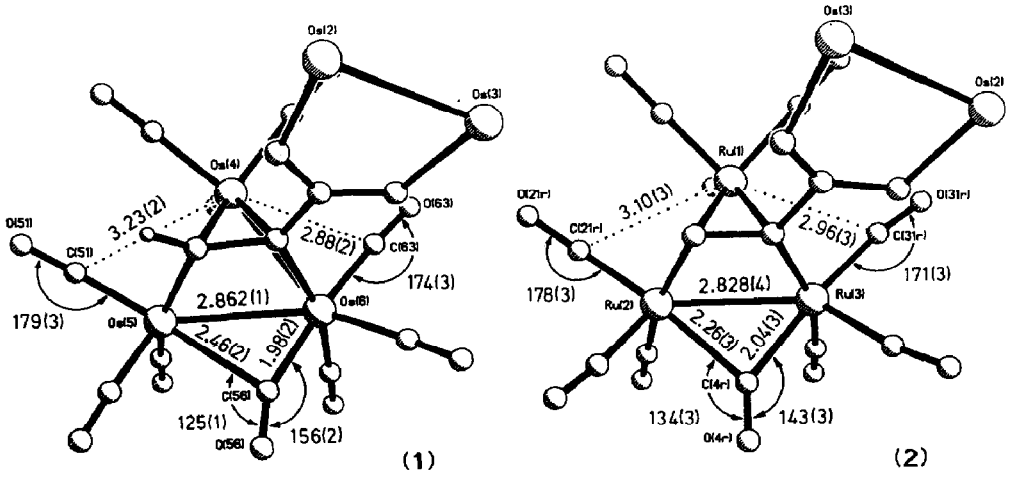

Fig. 4. A comparison of the geometries of the bridging CO ligands in the compounds **1** and **2** with an illustration of how the CO ligands *trans* to the CO bridges adjust their positions to remain closely *trans* to the bridge leading to approach to the third metal atom. (Distances in Å, angles in degrees).

the compounds $[Os_3(CO)_{10}(alkyne)]$ where alkyne = PhC_2Ph [2], HC_2Fc [3], and EtC_2Et [4] and in the PPh_3-substituted derivative of the latter [4]. This distortion from the strictly parallel arrangement is irrespective of whether there is a bridging carbonyl ligand present or not.

Figure 4 contains a comparison of the distribution of CO ligands around the related Os_3 and Ru_3 clusters presented here. Both could be said to have bridging CO ligands unlike $[Os_3(CO)_{10}(PhC_2Ph)]$ which does not. As might be expected the CO ligand is much closer to symmetrical in **2** than in **1**, the lighter metal being expected to accommodate bridging CO ligands more easily. In view of the non CO-bridged structure adopted by the PhC_2Ph compound we questioned whether there were two distinct structures or a continuum of structures. Figure 5 shows a plot of long against short M–C bond lengths in the CO bridge for the structurally established compounds. Although two compounds have non-bridged geometries and all the other ones have bridged geometries, these data seem to be more consistent with a continuum of structures rather than just two extreme types. It can be clearly seen that **1** is closer to the non-bridged form than is **2**. All six structures deviate from the as yet unobserved idealised symmetrical CO-bridged form indicated. There is also some correlation between the lowest observed ν(CO) wavenumber for each (that associated with the bridging or semi-bridging CO) and the CO geometry except that the triruthenium compound **2** has a higher value than the other bridged forms even though it is the most symmetrical. Ruthenium and osmium have different properties with respect to bonding to CO and there is no reason to expect the osmium and ruthenium infrared data to fit. The structures of **1** and **2** represent the first geometric comparison of Os and Ru in this series.

There is a good correlation of the geometry of the bridging CO and the M–M distance which it spans. Figure 6(a) shows the relation between the longer M–C distance in the bridge and the M–M distance while Fig. 6(b) shows a similar plot of the difference between the two M–C–O angles in the bridge against M–M distance. Both correlations are good. The variation of M–M distance over this series is only

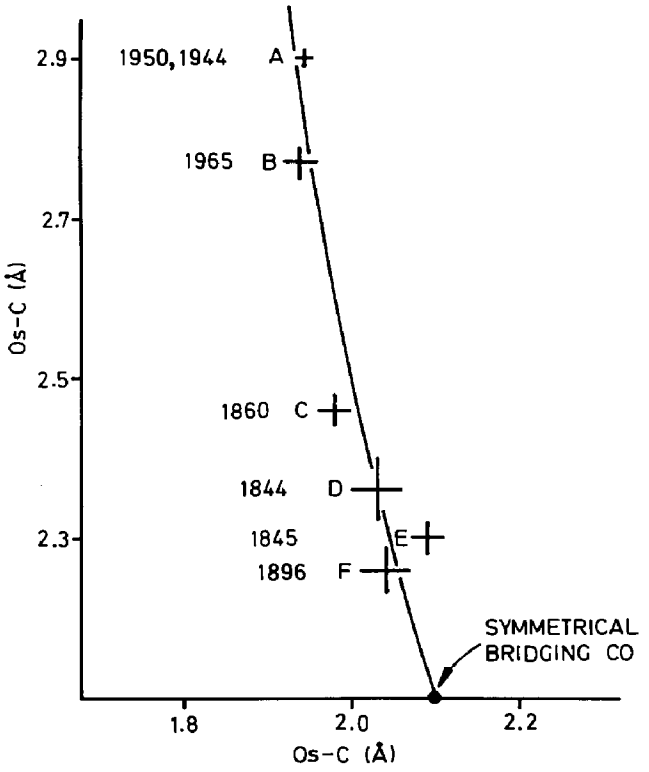

Fig. 5. Bond lengths for the bridging CO ligands for the compounds $[M_3(alkyne)(CO)_9L]$ (M = Ru or Os; L = CO or PPh_3): a graph of the longer M–C bond length in the bridge against the shorter M–C bond length. A $[Os_3(EtC_2Et)(CO)_9(PPh_3)]$ [4]; B $[Os_3(PhC_2Ph)(CO)_{10}]$ [2]; C compound **1**; D $[Os_3(HC_2Fc)(CO)_{10}]$; E $[Os_3(EtC_2Et)(CO)_{10}]$; F compound **2**. The lowest IR wavenumbers (cm^{-1}) for the CO ligands are given beside each point.

0.03 Å which is about a 2% variation. It is unreasonable to look for a cause for the gross change in CO geometries in this variation of M–M distances. More likely the steric or electronic effects that cause the structural variations have a major effect on M–C distances but only a minor effect on M–M distances. At this stage we cannot see any obvious electronic effects operating. The one known Ru compound fits in with the Os ones and it would be helpful to have some data for other compounds of this metal. We are planning to synthesise and determine the structures of other ruthenium compounds of the type $[Ru_3(CO)_{10}(alkyne)]$.

Experimental

Synthesis of compounds

The compounds $[Os_3H(CH{\equiv}CCO_2)(CO)_{10}]$ and $[M_3(CO)_{10}(CH{\equiv}CCO_2)$-$Os_3H(CO)_{10}]$ (**1**: M = Os; **2**: M = Ru) were synthesised as previously described [1].

Decarbonylation of compound 1

An orange solution of $[Os_3(CO)_{10}(CH{\equiv}CCO_2)Os_3H(CO)_{10}]$ in octane was heated under reflux for 30 min by which time the colour had paled to yellow and the IR

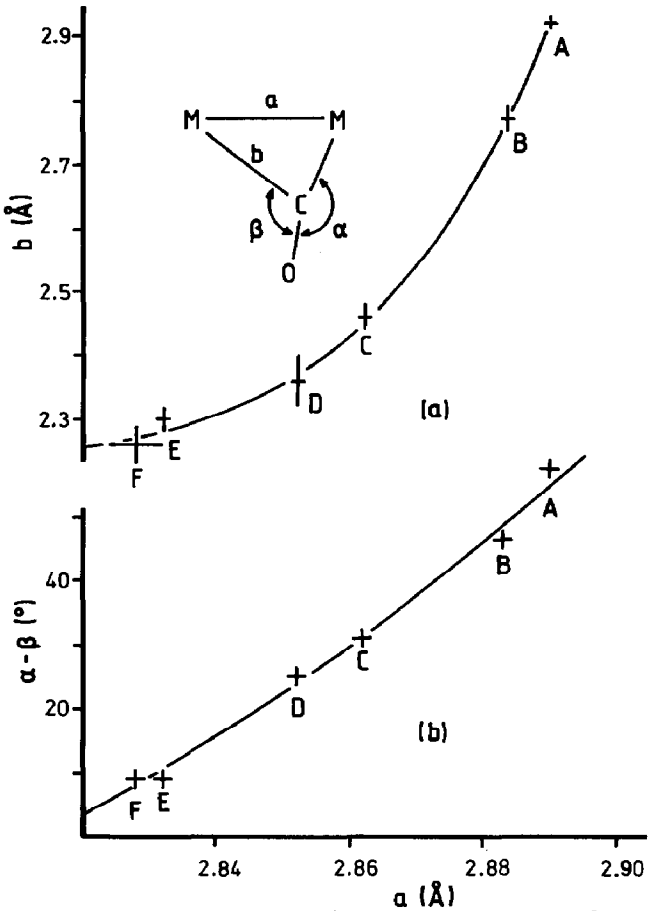

Fig. 6. Top plot (a): Graph of the long M–C distance b (Å) in the CO bridge against the bridged M–M distance a (Å). Bottom plot (b): Graph of the difference between the two M–C–O angles ($\alpha-\beta$) (°) in the CO bridge against the bridged M–M distance (a) (Å). Compounds labelled A to F are as in Fig. 5.

spectrum showed that complete reaction had occurred. TLC on silica (eluant light petroleum) gave one main yellow band which gave yellow crystals of $[Os_3H(CO)_9(C_3O_2)Os_3H(CO)_{10}]$ (**3**) in good yield. ν(CO) (cyclohexane): 2112w, 2104w, 2082vs, 2074s, 2063sh, 2058m, 2026vs, 2008s, 1992m cm^{-1}; ^1H NMR ($CDCl_3$): δ −10.4s and −23.2s. Single crystals of **3** suitable for X-ray crystal structure determination were obtained by evaporation of a pentane solution.

Decarbonylation of compound 2

A similar reaction of $[Ru_3(CO)_{10}(CH{\equiv}CCO_2)Os_3H(CO)_{10}]$ in cyclohexane under reflux for 50 min likewise gave the decarbonylation product $[Ru_3H(CO)_9(C_3O_2)Os_3H(CO)_{10}]$ (**4**) in good yield. ν(CO) (cyclohexane): 2114w, 2104w, 2084vs, 2078sh, 2063s, 2061sh, 2029vs, 2012s, 1998w, 1988w, cm^{-1}; ^1H NMR ($CDCl_3$): δ −10.45s and −21.15s.

Crystal structure determinations

Summarised X-ray crystallographic data for compounds **1**, **2**, and **3** are listed in Table 4. A crystal of each was mounted on a glass fibre on an Enraf–Nonius CAD4

Table 4

Crystallographic data for compounds **1** to **3**

	Compound **1**	Compound **2**	Compound **3**
Formula	$C_{23}H_2O_{22}Os_6$	$C_{23}H_2O_{22}Os_3Ru_3$	$C_{22}H_2O_{21}Os_6$
M (g mol^{-1})	1771.46	1504.07	1743.45
Colour	red	orange	bright yellow
Size (mm^3)	0.24×0.26×0.09	0.35×0.13×0.03	0.16×0.52×0.10
Crystal system	monoclinic	orthorhombic	triclinic
Space group	$P2_1/c$	$Pna2_1$	$P\bar{1}$
a (Å)	17.981(3)	25.177(1)	13.255(3)
b (Å)	8.918(1)	14.628(3)	13.998(4)
c (Å)	23.772(5)	9.398(2)	9.432(1)
α (°)	90	90	106.57(2)
β (°)	115.85(2)	90	92.05(2)
γ (°)	90	90	87.99(2)
U (Å^3)	3430.7	3461.1	1675.8
Z	4	4	2
D_c (g cm^{-3})	3.43	2.89	3.45
μ(Mo-K_α) (cm^{-1})	222.6	123.2	227.8
F(000)	3088	2704	1516
Radiation, λ (Å)	Mo, 0.71073	Mo, 0.71073	Mo, 0.71073
Temp. (°C)	25	25	25
Scan mode	ω	ω	ω
Maximum 2θ (°)	50	60	50
Total no. data	6634	5150	6156
No. unique data	6452	5150	5877
Structure solution	Patterson	Patterson	Patterson
Rejection criterion	$F_o \leq 3\sigma(F_o)$	$F_o \leq 3\sigma(F_o)$	$F_o \leq 3\sigma(F_o)$
No. reflns used in refinement	3910	2944	4788
Parameters refined	235	235	227
R	0.042	0.052	0.036
R_w	0.047	0.067	0.048
Weight w in weighting scheme	$4F_o^2/[\sigma^2(F_o)]^2$	$4F_o^2/[\sigma^2(F_o)]^2$	$4F_o^2/[\sigma^2(F_o)]^2$
Max. shift/e.s.d. in final refinement	0.01	0.01	0.04
Max. height in final diff. Fourier (eÅ^{-3})	1.22	1.52	2.84

diffractometer operating with graphite-monochromated Mo-K_α radiation. Unit cells were obtained by least-squares refinement of 25, 25, 22 reflections respectively in the 2θ ranges 14 to 30°, 14 to 28°, and 12 to 28° for **1**, **2**, and **3**, respectively.

Intensity data for the 6634, 5150, and 6156 reflections measured for **1**, **2**, and **3** in the 2θ ranges up to 50, 60, and 50°, respectively, were corrected for Lorentz and polarisation effects and a decay correction was applied based on the intensities of three standard reflections collected periodically throughout the experiment. The three sets of data were also corrected for absorption by the ψ-scan method and in the case of **2** a secondary extinction correction was also applied [9].

Structures were solved by the Patterson method in each case (SHELX-86 [10]) which revealed the positions of the metal atoms and the remaining atoms were

Table 5

Fractional atomic coordinates for $[Os_3(CO)_{10}(CHCCO_2)Os_3H(CO)_{10}]$ compound **1**

	x	*y*	*z*
Os1	0.84894(5)	1.0801(1)	0.26726(4)
Os2	0.79780(4)	0.7747(1)	0.24340(3)
Os3	0.92954(4)	0.8630(1)	0.36332(3)
Os4	0.65292(5)	0.6244(1)	0.40499(4)
Os5	0.53956(5)	0.8469(1)	0.38959(4)
Os6	0.71117(5)	0.8928(1)	0.46959(3)
O1	0.7277(7)	0.803(2)	0.2947(6)
O2	0.8290(7)	0.859(2)	0.3883(6)
O11	0.935(1)	1.360(2)	0.3369(8)
O12	0.975(1)	1.024(3)	0.2134(9)
O13	0.734(1)	1.212(2)	0.1403(8)
O14	0.7272(9)	1.142(2)	0.3246(7)
O21	0.652(1)	0.876(3)	0.1265(9)
O22	0.896(1)	0.711(2)	0.1714(8)
O23	0.735(1)	0.455(2)	0.2342(8)
O31	1.009(1)	0.612(3)	0.4584(9)
O32	1.078(1)	0.858(3)	0.3356(9)
O33	1.005(1)	1.126(2)	0.4509(8)
O41	0.805(1)	0.455(3)	0.417(1)
O42	0.615(1)	0.458(3)	0.500(1)
O43	0.550(1)	0.422(3)	0.297(1)
O51	0.408(1)	0.630(3)	0.309(1)
O52	0.492(1)	0.820(3)	0.498(1)
O53	0.435(1)	1.114(3)	0.3220(9)
O56	0.614(1)	1.186(2)	0.4195(8)
O61	0.843(1)	1.121(3)	0.4876(9)
O62	0.686(1)	0.955(2)	0.5883(9)
O63	0.844(1)	0.657(3)	0.544(1)
C1	0.610(1)	0.821(2)	0.3377(9)
C2	0.694(1)	0.831(2)	0.3791(8)
C3	0.754(1)	0.829(2)	0.3526(8)
C11	0.905(1)	1.253(3)	0.311(1)
C12	0.929(1)	1.035(3)	0.237(1)
C13	0.779(1)	1.166(3)	0.188(1)
C14	0.770(1)	1.113(3)	0.301(1)
C21	0.707(1)	0.845(3)	0.172(1)
C22	0.857(1)	0.736(3)	0.197(1)
C23	0.762(1)	0.573(3)	0.239(1)
C31	0.979(1)	0.708(3)	0.423(1)
C32	1.021(1)	0.856(3)	0.348(1)
C33	0.977(1)	1.025(3)	0.4191(9)
C41	0.746(2)	0.515(3)	0.412(1)
C42	0.630(1)	0.517(3)	0.464(1)
C43	0.590(1)	0.496(3)	0.340(1)
C51	0.459(1)	0.712(3)	0.340(1)
C52	0.508(2)	0.825(4)	0.456(1)
C53	0.471(2)	1.007(3)	0.347(1)
C56	0.634(1)	1.061(3)	0.4303(9)
C61	0.796(1)	1.035(3)	0.4807(9)
C62	0.697(1)	0.939(3)	0.542(1)
C63	0.791(2)	0.748(3)	0.511(1)
H1	0.571	0.824	0.286
H2	0.888	0.699	0.311

Table 6

Fractional atomic coordinates for $[Ru_3(CO)_{10}(CHCCO_2)Os_3H(CO)_{10}]$, compound **2**

	x	*y*	*z*
Os1	0.09526(4)	0.62814(8)	0.2328(2)
Os2	0.13872(4)	0.45565(7)	0.3200 [a]
Os3	0.15031(4)	0.51799(7)	0.0285(2)
Ru1	0.35785(9)	0.4634(2)	0.1791(3)
Ru2	0.40724(8)	0.6272(2)	0.2276(3)
Ru3	0.34558(9)	0.5427(2)	0.4420(3)
O1	0.2182(6)	0.507(1)	0.338(2)
O2	0.2243(7)	0.563(1)	0.111(2)
O4R	0.370(1)	0.743(2)	0.494(4)
O11R	0.274(1)	0.313(2)	0.165(3)
O11O	0.067(1)	0.794(2)	0.060(4)
O12R	0.457(1)	0.351(2)	0.234(4)
O12O	−0.005(1)	0.533(2)	0.131(3)
O13R	0.359(1)	0.442(2)	−0.141(4)
O13O	0.044(1)	0.684(2)	0.517(4)
O14O	0.199(1)	0.716(2)	0.321(4)
O21O	0.182(1)	0.266(2)	0.395(3)
O21R	0.458(1)	0.589(2)	−0.058(4)
O22O	0.028(1)	0.372(2)	0.309(3)
O22R	0.515(1)	0.614(2)	0.380(3)
O23O	0.124(1)	0.525(2)	0.620(3)
O23R	0.408(1)	0.825(2)	0.157(4)
O31O	0.217(1)	0.401(2)	−0.178(4)
O31R	0.306(1)	0.351(2)	0.504(4)
O32R	0.442(1)	0.509(2)	0.637(3)
O32O	0.052(1)	0.433(2)	−0.087(3)
O33R	0.259(1)	0.605(2)	0.647(4)
O33O	0.143(1)	0.681(2)	−0.167(3)
C1	0.329(1)	0.608(2)	0.151(3)
C2	0.302(1)	0.564(2)	0.257(3)
C3	0.243(1)	0.541(2)	0.228(3)
C4R	0.371(1)	0.676(2)	0.434(4)
C11R	0.308(1)	0.365(2)	0.175(4)
C11O	0.078(2)	0.733(3)	0.122(4)
C12R	0.417(1)	0.390(2)	0.232(5)
C12O	0.033(1)	0.565(2)	0.161(4)
C13R	0.358(1)	0.453(2)	−0.013(4)
C13O	0.066(1)	0.661(2)	0.419(4)
C14O	0.159(1)	0.681(2)	0.283(4)
C21O	0.170(1)	0.341(2)	0.373(4)
C21R	0.438(1)	0.603(2)	0.056(4)
C22O	0.070(1)	0.406(2)	0.311(4)
C22R	0.476(1)	0.619(2)	0.324(4)
C23O	0.130(1)	0.497(2)	0.511(4)
C23R	0.408(1)	0.753(2)	0.192(4)
C31O	0.192(1)	0.444(2)	−0.104(4)
C31R	0.322(1)	0.419(2)	0.471(4)
C32R	0.406(1)	0.521(2)	0.570(3)
C32O	0.089(1)	0.468(2)	−0.038(3)
C33R	0.294(2)	0.587(3)	0.571(5)
C33O	0.145(2)	0.621(3)	−0.081(5)

[a] Fixed.

Table 7

Fractional atomic coordinates for $[Os_3H(CO)_9(CCCO_2)Os_3H(CO)_{10}]$, compound **3**

	x	*y*	*z*
Os1	−0.26716(4)	0.22247(4)	−0.49406(5)
Os2	−0.42720(4)	0.34663(4)	−0.33908(6)
Os3	−0.24984(4)	0.30090(4)	−0.17811(5)
Os4	−0.25012(4)	0.73520(4)	−0.02256(5)
Os5	−0.23661(4)	0.81836(4)	−0.26499(6)
Os6	−0.08899(4)	0.67580(4)	−0.21962(5)
O1	−0.3457(6)	0.4789(7)	−0.3146(9)
O2	−0.2111(6)	0.4473(6)	−0.1866(9)
O11	−0.0671(9)	0.112(1)	−0.547(2)
O12	−0.3735(9)	0.034(1)	−0.477(1)
O13	−0.3391(9)	0.178(1)	−0.817(1)
O14	−0.1746(8)	0.4131(9)	−0.520(1)
O21	−0.4969(8)	0.3574(9)	−0.641(1)
O22	−0.5562(8)	0.1719(9)	−0.352(1)
O23	−0.580(1)	0.485(1)	−0.148(2)
O31	−0.2428(9)	0.378(1)	0.160(1)
O32	−0.3197(8)	0.1068(9)	−0.149(1)
O33	−0.0292(9)	0.232(1)	−0.204(1)
O41	−0.2199(8)	0.6230(9)	0.214(1)
O42	−0.231(1)	0.946(1)	0.186(2)
O43	−0.4788(9)	0.742(1)	−0.009(1)
O51	−0.4448(9)	0.914(1)	−0.251(1)
O52	−0.116(1)	0.999(1)	−0.110(2)
O53	−0.1846(9)	0.835(1)	−0.567(1)
O61	0.0343(8)	0.5113(9)	−0.136(1)
O62	0.0797(9)	0.824(1)	−0.156(1)
O63	−0.0481(8)	0.6036(9)	−0.549(1)
C1	−0.2551(8)	0.6814(9)	−0.270(1)
C2	−0.2322(8)	0.6044(9)	−0.219(1)
C3	−0.2648(9)	0.502(1)	−0.239(1)
C11	−0.142(1)	0.151(1)	−0.526(2)
C12	−0.332(1)	0.107(1)	−0.477(2)
C13	−0.311(1)	0.192(1)	−0.694(2)
C14	−0.210(1)	0.346(1)	−0.506(2)
C21	−0.473(1)	0.356(1)	−0.527(1)
C22	−0.501(1)	0.238(1)	−0.354(2)
C23	−0.525(1)	0.437(1)	−0.221(2)
C31	−0.244(1)	0.354(1)	0.029(2)
C32	−0.287(1)	0.182(1)	−0.161(2)
C33	−0.114(1)	0.260(1)	−0.197(2)
C41	−0.239(1)	0.667(1)	0.123(2)
C42	−0.237(1)	0.866(1)	0.105(2)
C43	−0.391(1)	0.741(1)	−0.014(2)
C51	−0.361(1)	0.885(1)	−0.256(2)
C52	−0.166(1)	0.935(1)	−0.174(2)
C53	−0.205(1)	0.829(1)	−0.450(2)
C61	−0.010(1)	0.572(1)	−0.162(2)
C62	0.012(1)	0.771(1)	−0.183(2)
C63	−0.063(1)	0.630(1)	−0.423(2)
H1	−0.384	0.343	−0.152
H2	−0.110	0.729	−0.019

located in succeeding difference Fourier syntheses. Hydrogen atoms were located for compounds **1** and **3** and added to the structure factor calculations but their positions were not refined. Metal atoms in each case were refined anisotropically. The structures were refined by full-matrix least-squares where the function minimised was $\Sigma w(|F_o| - |F_c|)^2$. Scattering factors and $\Delta f'$ and $\Delta f''$ were obtained from standard sources [11]; anomalous dispersion effects were included in F_c [12]. Details including the values of R and R_w, final shift/e.s.d values, and maximum residual peaks are in Table 4. Fractional atomic coordinates are in Tables 5 to 7. The absolute stereochemistry of compound **2** in the crystal was not determined; such compounds would rapidly racemize in solution.

All computations were carried out using a MicroVax II computer using SDP/VAX [13].

Acknowledgements

We thank the SERC for a studentship (for N.I.P.), the NSF for a diffractometer grant, and NATO for support for this collaboration.

References

1 A.J. Arce, Y. De Sanctis, and A.J. Deeming, Polyhedron, 7 (1988) 979.
2 M. Tachikawa, J.R. Shapley, and C.G. Pierpont, J. Am. Chem. Soc., 97 (1975) 7172; C.G. Pierpont, Inorg. Chem., 16 (1977) 636.
3 K.I. Hardcastle, A.J. Deeming, D. Nuel, and N.I. Powell, J. Organomet. Chem., 375 (1989) 217.
4 E. Rosenberg, J. Bracker-Novak, R.W. Gellert, S. Aime, R. Gobetto, and D. Osella, J. Organomet. Chem., 365 (1989) 163.
5 G.A. Foulds, B.F.G. Johnson, and J. Lewis, J. Organomet. Chem., 296 (1985) 147.
6 S. Rivomanana, G. Lavigne, N. Lugan, J.-J. Bonnet, R. Yanez, and R. Mathieu, J. Am. Chem. Soc., 111 (1989) 8959.
7 J.R. Shapley, G.M. St. George, M.R. Churchill, and F.J. Hollander, Inorg. Chem., 21 (1982) 3295.
8 S. Aime and A.J. Arce, unpublished results.
9 W.H. Zachariasen, Acta Crystallogr., 16 (1963) 1139.
10 G.M. Sheldrick, SHELX-86, Program for Crystal Structure Solution, University of Göttingen, 1986.
11 D.T. Cromer and J.T. Waber, International Tables for X-Ray Crystallography, Vol IV, The Kynoch Press, Birmingham, England, 1974, Table 2.2B.
12 D.T. Cromer, Ref. 11, Table 2.3.1.
13 B.A. Frenz, in H. Schenck, R. Olthof-Hazelkamp, H. van Konigsveld, and G.C. Bassi (Eds.), Computing in Crystallography, Delft University Press, Delft, 1978, p. 64–71.